

# **Chapter I**

## **Introduction**

### **RESUMEN**

La introducción se encuentra dividida en cinco secciones. En la primera sección se introducen los conceptos físicos referidos a la medida de la calidad óptica de la imagen en el ojo humano, así como algunas definiciones, terminología y convenios usados en esta tesis. En la segunda sección se introducen los métodos usados para medir las aberraciones totales y corneales (las técnicas usadas y desarrolladas en esta tesis se presentan en el capítulo II. La sección tercera presenta el estado del arte del conocimiento de las contribuciones corneales e internas a la calidad de imagen retiniana en ojos normales. En la sección cuarta se introducen brevemente algunas de las situaciones clínicas y oftálmicas en las que se aplicará la medida de aberraciones, tales como procedimientos de corrección de ametropías (cirugía refractiva corneal, cirugía de implante de lentes intraoculares, uso de lentes de contacto), la miopía, la afaquia o patología de queratocono. Finalmente, en la quinta sección se exponen los objetivos concretos que se abordarán en la tesis.

**ABSTRACT**

The introduction is divided in five sections. Section 1 introduces the physical concepts related to the measurement of the image quality in the human eye as well as the definitions, terminology and conventions used in this thesis. Section 2 introduces current methods to measure total and corneal aberrations (the techniques used and developed in this thesis will be presented in Chapter 2). Section 3 presents briefly the state-of-art of corneal and internal contributions to retinal image quality in the normal eye. Section 4 introduces briefly some of the clinical and ophthalmic situations where aberration measurements will be applied, such as correction procedures (corneal refractive surgery, surgery with intraocular lens implant and contact lenses) or in conditions such as myopia, aphakia, or keratoconus. Finally, section 5 presents the goals of the thesis.

Optical aberrations show the departure of the eye from a perfect optical system. Historically, measurements of aberrations in the human eye were restricted to the assessment of defocus and astigmatism, i.e. low order aberrations that can be corrected by conventional spectacles. It has not been until the last decades when the rapid increase of aberration measurement technology has allowed to measure higher order aberrations. In addition to aberrometry of the global eye, the development of accurate measurements of the corneal shape has led to the first detailed analysis of the optical contribution of the different ocular elements, which opens a wide range of basic and clinical applications. In fact, these advances have started to cause an important impact in the ophthalmology practice. One of the most useful applications of these technologies occurs in corneal laser surgery and cataract surgery. Measurement of the increase of aberrations induced by these surgeries has revealed issues that cannot be accounted for using classical refraction measurements. Furthermore, these type of measurements has opened the possibility of improving surgery, by optimizing the design of the intraocular lenses implanted in cataract surgery or by customization of laser ablation algorithms in corneal surgery. Moreover new technologies to correct eye aberrations have arisen with two fundamental goals: the improvement of visual quality and the increase of resolution of retinal imaging devices.

The research conducted in this thesis has run parallel to complementary research in other national and international laboratories. All these developments have turned the field in an increasing relevant area of vision, with impact in the clinic and industry. In this thesis, we analyze the contribution of the different ocular components to ocular aberrations in different clinical situations, for a better understanding and possible improvement of treatments.

# 1. Image formation in the human eye

## 1.1 Optical transfer function and wave aberration.

The optical system of the eye projects the images of objects onto the retina, where light is captured by the photoreceptors and converted into neuro-electrical signals transmitted to later stages of the visual process. Due to the wave nature of light and diffraction effects produced by the limited circular aperture of the pupil, the best image of a point source projected on the retina by the optics of the eye is the diffraction-limited Airy disc. Optical aberrations and scattering distort the image of a point source from the Airy disc. The *Point Spread Function (PSF)* is defined as the distribution of the radiation in the retina of an object point. For an extended object represented by a spatial function:  $o(x,y)$ , the distribution of light in the retina  $i(x',y')$  can be generalized as follows:

$$I(x',y') = O(x,y) \otimes PSF(x',y')$$

Thus the image formation of the human eye at the retina is fully described by a mathematical operation called convolution (represented by  $\otimes$ ), given the PSF of the eye. Using Fourier operations, convolution is transformed to a multiplication in the frequency domain:

$$I(u',v') = O(u,v) * OTF(u',v')$$

Where *OTF* is the *Optical Transfer Function* that measures the contrast degradation of the different frequency components imposed on object  $(u,v)$  by the optical system. The OTF is a complex function where the modulus is the *modulation transfer function (MTF)* and its phase is the *phase transfer function (PTF)*.

Following scalar diffraction theory (ignoring polarization<sup>a</sup>) of wave propagation

---

<sup>a</sup> Ocular media have some degree of anisotropism giving rise to birefringence properties, specially at the cornea because of the particular distribution of the collagen. Although these *polarization* properties of the eye must be considered for analysis of image reflected by the retina in ophthalmic instrumentation, it has been proved that their effects on the image retinal quality are negligible<sup>1,2</sup>.

and using Fraunhofer approximation the point spread function is given by<sup>3</sup>:

$$PSF(x', y') = cte * \left| FT \left\{ T(x, y) * e^{-i(2\pi/\lambda)WA(x,y)} \right\} \right|^2$$

Where  $T(x,y)$  is the transmittance pupil function,  $WA(x,y)$  is the **wave aberration** function and  $(x,y)$  are coordinates in the pupil plane. In the present thesis we will assume that the transmittance pupil function is constant (i.e., the apodization effect by cone-directionality<sup>4, 5</sup> is not considered). In the absence of scattering, the PSF of the human eye can be obtained directly from the wave aberration for any given pupil size.

Wave aberrations can be also defined using geometrical optics. A geometrical optics model assumes that light can be represented as ray propagation following trajectories according to Fermat's principle.

J.C. Maxwell defined the ideal optical system as that for which<sup>6</sup> all rays coming from a point O (object point) in a defined plane x-y (object plane) pass through a point O' (image point) in a plane x'-y' named image plane. Another condition required for the "ideal" optical system is that coordinates (x',y') of image point must be proportional to (x,y). The constant of proportionality is named magnification. The eye is not an ideal optical system, since it suffers from aberrations that deflect the rays from the ideal location. The **wavefront** is defined as the surface of constant optical path -the optical path is the physical path multiplied by the medium refractive index- from a point source; considering Malus-Dupin theorem the wavefront is always a surface orthogonal to the rays coming from the source point<sup>7</sup>. For an ideal point image the ideal wavefront is a spherical surface. The **wave aberration** is defined as the optical path surface difference from an ideal spherical wavefront.

## 1.2 Aberrations in the human eye

**Aberrations** of an optical system can be defined as the deviation of the rays from their ideal trajectories as defined above. Aberrations can be expressed in three different ways<sup>8</sup>: Longitudinal, transverse and wave aberration. A schematic diagram of the relations between these definitions is illustrated in Figure I.1.

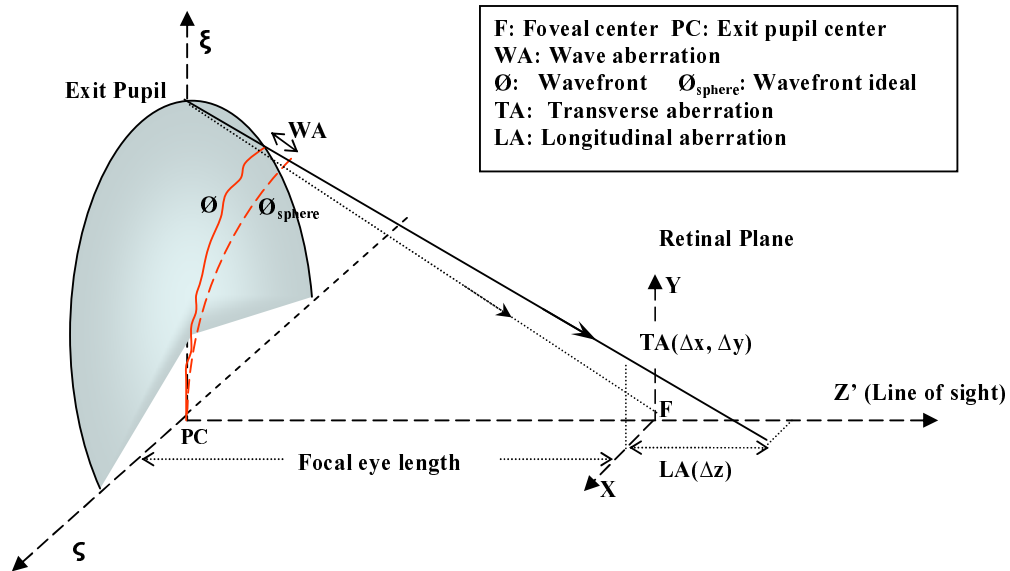


**Figure I.1:** Wave, transverse and longitudinal aberration of a ray in a simplified scheme of the human eye considering only the exit pupil and the image plane. The image plane is located at the retinal surface. The exit pupil is determined by the image of the iris stop through the crystalline lens. The line of sight is the axis passing through the center of the eye pupil and the object point. Transverse aberration for the ray in the figure is determined by the coordinates  $\Delta x$ ,  $\Delta y$  of the intersection of the ray with the retina plane; longitudinal aberration is determined by coordinate  $\Delta z$ .

Experimentally one typically measures the transverse aberration (TA) which is related by first derivatives to the wave aberration (WA)<sup>9</sup> for different pupil positions.

Aberration theory has been widely studied in rotationally symmetric systems for optical design and testing purposes<sup>6, 10</sup>. In conventional optical systems, analytical expressions of aberrations can be obtained as a function of a few parameters such as radius, asphericities, thickness of surfaces and index of the media<sup>6</sup>. However the optical system of the eye is composed of complex and non-symmetrical surfaces, and in general, accurate information of the optical and geometrical properties of the ocular surfaces is limited. The wave aberration of the optical system of the eye is therefore typically obtained by means of a discrete sampling and measurement of a set of local aberrations, which are then fit to a functional expansion of the wave aberration.

Aberrations are usually referred with respect to the optical axis. However in the human eye, the centers of curvature of the cornea, crystalline lens surfaces and the pupil center are not aligned, and therefore an unique optical axis cannot be defined. The

aberrations of the eye are generally referred to the line of sight (axis joining the object fixation point with the entrance pupil center)<sup>11</sup>. The pupil stop in the human eye is set by the iris, so the entrance pupil is the image of the physiological pupil through the cornea. The exit pupil is not as easy to localize as the entrance pupil so it is also recommended to refer aberrations to the entrance pupil<sup>11</sup>.

### 1.3 Zernike representation of wave aberrations

As the wave aberration depends not only on pupil coordinates but also on object coordinates, there are two representations for the wave aberration: including explicitly the dependence of object coordinates (i.e. classical Seidel aberrations), or assuming implicitly the object position and including only dependence on pupil coordinates. For the human eye the second type of representation is typically used, considering a point object at infinity.

The wave aberration is in general a complex surface function, and it is usually described as a polynomial expansion. Howland et al<sup>12</sup> proposed a Taylor expansion to describe the wave aberration function in terms of pupil coordinates. Zernike polynomial expansion has become, however, the standard to represent ocular wave aberration data. Zernike polynomials were first introduced by Frits Zernike in interferometric contrast-phase microscopy<sup>13</sup>. The main advantage of the set of Zernike polynomials is that they are orthonormal in a unit circle. As pupil coordinates are usually normalized for a unit circle, any continuous wave aberration function can be expressed in terms of a Zernike expansion. Another advantage is that some Zernike polynomials can be related easily to magnitudes typically used in optometry, such as defocus or astigmatism. Each Zernike term is formed by the product of a radial, an angular function and a normalization factor. Each term is specified by a radial  $n$  and an angular  $m$  indexes. The Zernike coefficients represent the contributions of each specific term to the wave aberration. The Optical Society of America has established a set of recommendations<sup>14</sup> (sign, normalization and ordering) for reporting the Zernike polynomials which we will follow in this thesis. OSA notation uses Noll's normalization<sup>15b</sup> and also proposes an alternative

---

<sup>b</sup> Noll's normalization forces the different Zernike terms to have the same variance equal to 1. Thus the total variance of the wave aberration is the sum of the squares of the coefficients of the Zernike terms.

single scheme notation with a index  $j$  formed from  $n$  and  $m$ :

$$j = \frac{n(n+2)+m}{2}$$

In certain applications it is interesting to refer the aberrations in terms of classical power series expansion. Each Zernike term usually contains different powers. For example  $Z_4^0 = \sqrt{5}(6\rho^4 - 6\rho^2 + 1)$  is a balance of spherical primary aberration, term  $\rho^4$ , and paraxial defocus term  $\rho^2$ , and piston, term 1. Matrix transformation between classical power-series expansion and Zernike aberrations can be found in several optics manuals<sup>16</sup>. The order of the Zernike terms is given by the power of  $\rho$ . For  $n=0$  the  $Z_0^0$  term is a constant (piston) added to the global wavefront, and does not affect optical quality. For  $n=1$ ,  $Z_1^{-1}$  and  $Z_1^1$  are referred as tilt terms. Tilt only produces a global shift of the retinal image affecting image position but no image shape. In foveal vision, the eye places the image at the fovea, canceling tilt effects. In the present thesis we use in most cases a 7<sup>th</sup> order Zernike polynomial expansion, where piston and tilt terms will be ignored in all cases.

Figure I.2 shows the first fifth orders (without piston & tilts) in the Zernike expansion and the corresponding retinal PSF (for values of the Zernike coefficients equal to  $\lambda$ ).



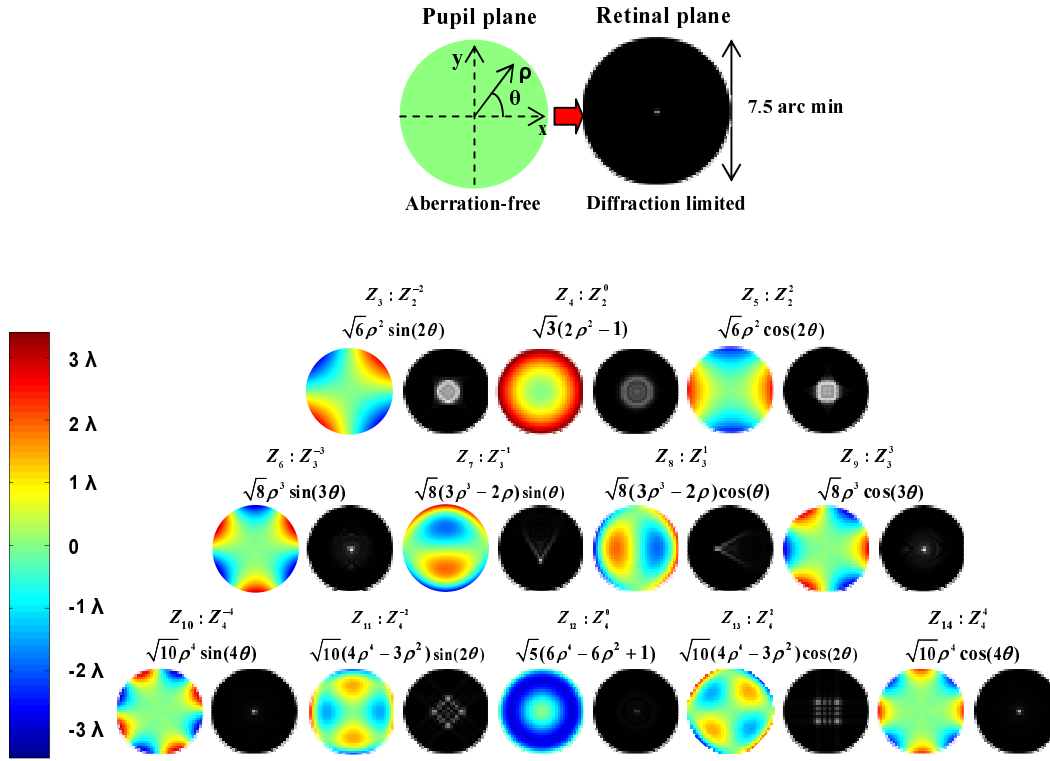


**Figure I.2:** Zernike polynomial terms and the corresponding retinal PSFs. The top figure represents a diffraction limited case. The pupillary image shows the axis and angular convention. The pyramidal representation shows 2<sup>nd</sup> to 4<sup>th</sup> order polynomials, and their corresponding PSF for all  $W = \lambda$ . The scale of the pupillary wave aberrations is in microns (for  $\lambda = 0.555$ ) and the scale of the retinal images is in arcmin. The first three aberrations (piston and tilts, i.e. 0 and 1<sup>st</sup> orders) are omitted. Note that piston has been adjusted to give a null value of wave aberration in the central pupil position.

#### 1.4 Global metrics to evaluate optical quality in the human eye

The wave aberration is described by a set of Zernike coefficients (typically 37 in this thesis). In many applications it is useful to characterize the wave aberration in terms of a single number which will represent a global image quality metric. One option it is to use the peak to peak wave aberration which is simply defined as the maximum departure of the wavefront from the ideal wavefront. A more complete metric is the root mean square wavefront error (RMS) defined as the root square of the variance of the wave aberration:

$$RMS = \sqrt{WA^2 - (\overline{WA})^2}$$

The RMS gives an average value of the magnitude of the wave aberration. The

orthogonal properties of the Zernike expansion and Noll's normalization allow to calculate easily the RMS as the square root of the sum of Zernike coefficients squares.

Global image quality will be described in this thesis in terms of the RMS, and the contribution of specific order terms as the RMS corresponding to those orders (i.e. setting the rest of Zernike coefficients to zero). It should be noted that RMS is a pupil plane optical quality metric and does not necessarily correlate highly with visual performance metrics such as visual acuity or subjective refraction<sup>17</sup>, among other reasons, because it does not take into account diffraction and scattering. Other metrics based on retinal images (i.e. PSF or MTF) can also be used. When considered necessary, in this thesis we also provide estimations of the Modulation Transfer Functions (MTF) computed from the wave aberration.

Figure I.3 shows how aberrations change the size and shape of the PSF for different eyes measured in this thesis.

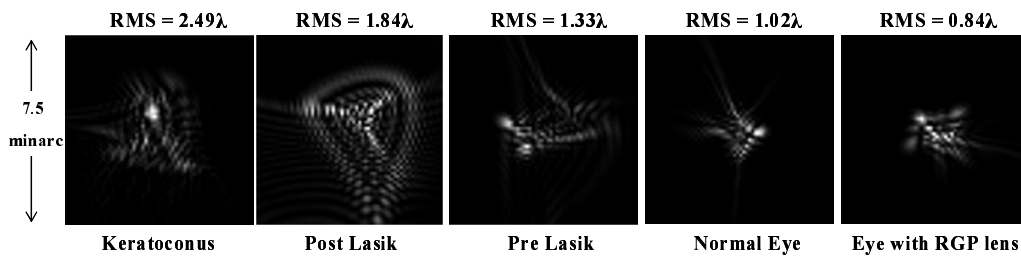


**Figure I.3:** Point spread functions (PSF) for different eyes with different amounts of RMS (excluding tilts and defocus). It can be shown how in highly aberrated eyes, like keratoconus and post Lasik eyes, the PSF is more spread and distorted.

## 2. Aberration measurements in the human eye

The first objective evaluations of the optical quality of the human eye were performed using double-pass techniques. These techniques projected originally line light sources<sup>18</sup>, and later (with the availability of lasers) point light sources<sup>19</sup> on the retina. The aerial image projected from the retina back onto a CCD camera (the autocorrelation of the PSF<sup>20</sup>) was used to compute the MTF. Double-pass image quality contains information of optical quality degradation produced by diffraction, scattering and aberrations. However, this technique does not allow direct measurement of the wave aberration since phase information is lost, although there has been some attempts to retrieve wave aberrations from double-pass aerial images and MTFs using optimization algorithms<sup>21</sup>. Aberrometers or wavefront sensors allow direct measurements of the wave aberration in the pupil plane.

### 2.1 Measurements of total aberrations

Early direct measurements of aberrations in the pupil plane were performed psychophysically, using artificial pupils and evaluating the local diopter power of different regions across the pupil<sup>22</sup>. Berny et al<sup>23</sup> conducted the first objective measurement of wave aberration using the Foucault test; since then, different techniques have been developed. Most of them measure transverse aberrations and then estimate the wave aberrations.

One way to classify aberrometry is in psychophysical and objective techniques<sup>c</sup>. Psychophysical techniques need the collaboration of the subject and are based on Vernier alignments<sup>24-26</sup> or Tscherning test<sup>27</sup>. The first psychophysical methods were slow, but recently fast methods have been implemented (i.e. the spatially resolved refractometer)<sup>12, 28, 29</sup>.

Objective techniques can be divided in sequential or parallel wavefront sensors. Parallel aberrosopes only require capture of a single snapshot while sequential are

---

<sup>c</sup> Aberrosopes can also be classified depending on whether aberrations are measured in the first pass (called ingoing aberrometers such as the crossed cylinder aberroscope, laser ray tracing, spatially resolved refractometer) or in the second pass, as the light emerges from the eye (outgoing aberrometers such as the Hartmann-Shack).

based in a sequential laser ray tracing and capture of a sequence of images<sup>30, 31</sup>. The first objective “aberroscope” (parallel) for the human eye was developed by Walsh et al<sup>32</sup> in 1984, based on the crossed cylinder aberroscope of Howland et al<sup>33</sup>. Tscherning principle has been also implemented objectively<sup>34</sup>. Currently, the most popular parallel aberrosopes are those based on Hartmann-Schack wavefront sensors, originally used in astronomy and first used in the human eye by Liang et al<sup>35</sup>.

In the present thesis we have used a sequential objective aberroscope technique developed by Navarro et al<sup>30</sup>. In this technique the pupil is sampled by scanning a set of narrow laser beams and the corresponding aerial images reflected off the retina are sequentially captured by a CCD. The actual implementation of the systems used in this thesis will be described in chapter II.

## 2.2 Measurements of corneal aberrations

The radius of curvature of the cornea has been measured since long ago, by estimating the size of the images reflected from its surface. Also, it is known for more than a century<sup>36</sup> that natural cornea typically shows some degree of toricity, i.e.. the radius of curvature in vertical meridian is usually greater than in the horizontal meridian forcing an astigmatism “with the rule”. Moreover, the cornea presents an aspherical shape. This asphericity has been usually represented by a conicoid surface, with two parameters: apical radius and asphericity  $Q$ , —introducing toricity in this scheme the cornea would be represented by a biconiocid—. Normally, the cornea flattens with the distance from the surface apex leading to negative values for  $Q$ <sup>37-39</sup> and therefore showing lower values for spherical aberration than those exhibited by a perfect spherical surface. However, it has not been until recently, with the development of the videokeratoscopes, that spatially resolved corneal elevation maps of individual corneas can be obtained, and the shape of the cornea has been studied systematically. Accurate corneal elevation measurements are required to estimate the aberrations that are induced by the cornea. There are several optical techniques to measure corneal surface using specular reflection, diffuse reflection or scattered light<sup>40</sup>. Nowadays the majority of commercial videokeratoscopes are based on Placido disk specular reflection, or in slit-lamp (scattered light) systems. In the present thesis we use a Placido disk

videokeratoscope, whose principles and accuracy will be described in chapter II. There are also several mathematical reconstructions of the corneal wave aberration from the corneal elevation map. A comparison of the methods used by several authors with the method used in this thesis will be also presented in chapter II.

### **3. Sources of aberrations on the human eye**

The measurement of the aberrations of the normal eye is important to understand the quality of the retinal image, which limits the spatial information available to later stages in the visual process. Measuring aberrations in pathological eyes, or eyes after an ocular procedure is becoming a quantitative diagnostic and evaluation tool in the clinic. Furthermore, the knowledge of the optical aberrations of individual components of the eye will provide deeper insight into the sources of optical degradation of individual eyes.

The present thesis will measure the aberrations of the cornea and the internal media in different conditions. Knowledge of aberrations of individual ocular components will allow us to obtain information about the shapes of ocular surfaces (e.g. changes of the posterior corneal surface after corneal refractive surgery), relationships between the geometrical properties of intraocular lenses implanted in eyes after cataract surgery and their aberrations measured *in vivo*, or discuss properties such as the gradient index of the lens, among others. Current schematic eye models, based on simple surface models of the cornea and crystalline lens and average values of intraocular distances, have limited success in predicting individual values of optical properties in the human eye. For this reason individual information will be essential in customizing schematic eyes models, either in normal eyes or eyes with modified surfaces (such as the cornea after corneal refractive surgery), replaced surfaces (such as an intraocular lens) or added surfaces (such as contact lenses). The following are properties which will affect the measured aberrations of the whole eye, as well as the aberrations of the individual components.

### 3.1 Intraocular distances, tilts and decentrations.

The pupil of the eye is slightly displaced with respect to the rest of the center of the other ocular components by  $\sim 0.5$  mm<sup>41</sup>, on average across individuals. The position of the fovea is also shifted from the best fit optical axis by  $\sim 5^\circ$  on average toward the temporal side<sup>42</sup>. These are average values across the population (some of the studies are actually based on a small sample) and significant variability across eyes occurs. Shifts and tilts between ocular surfaces, fovea and pupil makes impossible to define a clear optic axis for the eye, presumably leading to the existence of coma-like aberrations and astigmatism even for on-axis objects as shown by eye models<sup>43</sup>; although it has been reported that by themselves these shifts and tilts are not the main sources in individual variations between monochromatic aberrations<sup>44</sup>.

Purkinje images (specular reflections from the different surfaces of a light point source) and Scheimpflug imaging can be used to measure tilts and decentrations between cornea and lens and also the fovea positioning<sup>45,46</sup>. Intraocular distances can be measured with different degrees of resolution by ultrasound biometry, such as A-scan ultrasonography, slitlamp biometry —specially Scheimflug photography—, partial coherent interferometry (PCI), or optical coherence tomography (OCT).

### 3.2 Surface shapes

The shape of the anterior surface of the cornea determines the corneal aberrations, and to a certain extent the ocular aberrations. However, total aberrations result from a combination of corneal and internal aberrations (the latter predominantly from the crystalline lens). To date, there is no systematic study that links the internal aberrations with the geometrical properties of the posterior surface of the cornea and the shapes of the crystalline lens.

As described previously there are multiple techniques to measure the shape of the anterior corneal shape, but it is not easy to measure internal surfaces of the eye in vivo because optical measurements are distorted by the optics of the cornea and subsequent surfaces. A first estimation of the average curvature of the surfaces can be performed by Purkinje images<sup>47</sup>. This technique has being used, for example, to assess the changes of curvature of the crystalline lens with refractive error and with accommodation<sup>48</sup>. The

posterior corneal surface has been evaluated with conventional slit lamp<sup>49</sup> or combining videokeratoscopy with pachymetric thickness<sup>50</sup>. However, to estimate asphericity, more sophisticated techniques are required. The Scheimpflug camera (a modified slit lamp with the image plane tilted with respect to the optical axis) allows capturing sections of the anterior segment with better resolution than conventional instruments. It has been used to measure asphericity in crystalline lens<sup>51</sup> and posterior cornea surface<sup>39</sup>, although this technique requires accurate correction for distortions and careful calibration. For this reason there are scarce, and sometimes controversial reports of the curvatures of the crystalline lens, and how they change with age, based on this technology.

Measurements on large populations of total<sup>52, 53</sup> and corneal<sup>54</sup> aberrations reveal a high variability in higher order aberrations across subjects. Thibos et al<sup>53</sup> on 100 eyes did not find systematic trends for third order aberrations, suggesting no presence of specific structure in ocular components in normal eyes. Surface individual irregularities have been suggested to explain high variability found in higher order aberrations between subjects<sup>44</sup>. The only systematic tendency has been found for spherical aberration showing typically positive values.

### 3.3 Refractive index

Apart from the geometry of the optical surfaces the distribution of refractive index inside the eye plays a fundamental role in its refractive properties.

Aqueous humour which fills the anterior chamber and vitreous humour, filling the vitreous chamber, are water solutions, and therefore their refractive indices are close to that of the water 1.336. The cornea is composed of several layers: tear film, epithelium, Bowman's membrane, stroma, Descemet's membrane and the endothelium, each of them with a different structure and therefore different refractive index. However to date there are not ideal methods available to measure accurately the refractive index of each layer<sup>55</sup>. As a result an "effective" refractive index is used to model the cornea (see discussion in chapter II, section 3.4).

The crystalline lens is a compact lens composed of an external epithelial layer and a nucleus-cortex made of fiber layers. Such structure shows a gradient-index distribution that it is expected to depend on several factors: accommodation state<sup>56</sup>, age<sup>56, 57</sup>, etc... A

detailed discussion of the gradient index distribution of the crystalline lens is presented in chapter VIII, where a technique to reconstruct the gradient is presented.

### 3.4 Combined measurements of corneal and total aberration

The measurement of the shapes and positions of the surfaces allows individual eye modelling and, assuming knowledge of refractive indices, an estimation of the ocular aberrations. More direct ways to evaluate the contribution of the cornea and the crystalline lens to overall image quality involve aberration measurements of both elements separately. Some imaginative approaches have been used. Young in 1901<sup>24</sup> tried to measure the optical properties of the human lens in vivo by canceling the corneal contribution immersing the human eye in water (whose refractive index is close to that of the cornea). This technique has been also used by Millodot et al<sup>58</sup> and by Artal et al<sup>59</sup>. Another approach is that from Tominsoln et al<sup>60</sup> who measured the contrast sensitivity of the eye combined with the modulation transfer of the cornea with different pupil sizes.

However, the most successful technique has been to measure total aberrations —with techniques as described in section 2.1— and corneal aberrations —from corneal elevation maps, as described in section 2.2— separately. This is the methodology that we use in the present thesis and will be explained in detail in chapter II. To our knowledge El Hage, and Berny<sup>61</sup> were the first ones to use this approach. They measured the corneal spherical aberration using photographic keratometry and a Foucault knife-edge test to measure spherical aberration of the total eye. They found a balance between the spherical aberration of cornea and that of the crystalline lens in a single subject. Since this first experiment in 1973, and with the advance of videokeratoscopy and aberrometry, the accuracy of the data and the increased number of experiments has shown interesting results. Artal et al<sup>59, 62</sup> reported a general compensation of higher order aberrations, not only spherical, that decrease with age<sup>63</sup>. Salmon and Thibos<sup>64</sup> presented data in three subjects, with two of them showing a certain degree of aberration balance, but not the other one. In the present thesis we present the interrelations between internal and corneal optics in the eyes of a monolateral aphakic eye (chapter IV), keratoconus eyes (chapter III), patients before



and after LASIK (chapter IV), patients before and after cataract surgery (chapter VII), and in a control group of young eyes.

## 4. Ophthalmic and clinical applications

Knowledge of aberrations is useful not only to understand the ocular system of the normal eye. Perhaps the ability to measure accurately the optical quality of the ocular components is most powerful in the study of abnormal ocular optics. The present thesis demonstrates that corneal topography and total aberrometry, and in particular the combination of both techniques, can be an important tool in studies on pathologies of the human eye, changes induced by refractive surgery, or design and in vivo testing of ophthalmic devices (i.e. intraocular lenses or contact lenses). Furthermore, the growing interest and applications of aberrometry has contributed to the advance of customized correction techniques with two mainly goals: to provide the eye with a better retinal quality, and a better vision as a consequence, and to improve the resolution in retinal imaging<sup>65, 66</sup>. The following subsections introduce some of the applications covered in the present thesis.

### 4.1 Biological, ocular changes and pathologies

#### *Aging*

The visual system degrades with age<sup>67, 68</sup>. While some of the changes are known to have a neural origin, part of the degradation is due to optical factors. Intraocular scattering increases with age<sup>69</sup>, and becomes impairing with the formation of cataracts. In addition, several recent studies have revealed an increase of total ocular aberrations with age<sup>63, 70, 71</sup>. This increase can be attributed to different factors: 1) An increase of corneal<sup>72</sup> and crystalline lens aberrations<sup>63, 73, 74</sup> with age. 2) A loss of the compensation between cornea and crystalline lens aberrations that occurs in the young eye<sup>59</sup>. The study of corneal and total aberrations in the aging eye is particularly relevant to understand the optical changes induced in cataract surgery (see chapter VII).

### ***Myopia***

The study of the optical aberrations in myopic eyes is interesting for two reasons. Firstly myopic eyes are known to have increased axial length, but there are few, and sometimes controversial data on the optical and geometrical properties of the ocular components in myopic eyes<sup>75</sup>. The success of different correction alternatives for myopia relies on an adequate knowledge of the optics of the myopic eye. Secondly, the etiology of myopia is not well understood. There is supported evidence, particularly from animal models, that emetropization (tuning of the focal length of the ocular optics to the axial length of the eye) is visually guided. It has been shown that an optical retinal image is required for proper emetropization, and that degraded retinal image (by diffusers, occluders, and perhaps aberrations) results in development of myopia<sup>76</sup>. Several studies show an increase of the amount of higher order aberrations in myopic eyes<sup>77-79</sup>, specially 3<sup>rd</sup> aberrations, while a certain degree of corneal/internal spherical aberration balance seems to hold in a wide range of refractive errors (0 to -16 D)<sup>78</sup>. The increase of corneal spherical aberration relates with increased corneal asphericity found in myopes<sup>80</sup>. However, the sources of increased negative spherical aberration of the crystalline lens or the interactions of corneal/internal aberrations requires further investigation<sup>81</sup>.

### ***Corneal pathologies***

Pathologies that affect corneal normal shape degrade corneal optical quality and consequently retinal image quality. Total and corneal aberrometers can therefore result in useful diagnostic tools in these types of pathologies. Relatively common corneal pathologies are Terrien's and Pellucid's marginal degenerations or keratoconus. Keratoconus is characterized by progressive thinning and steeping of the cornea, creating a characteristic cone-bulge shape in the corneal elevation map<sup>82</sup>. Increased corneal aberrations with respect to normal eyes have been reported in keratoconic eyes. The highest increase occurs in coma-like aberrations<sup>83, 84</sup>. An example of the technology developed in this thesis used in keratoconus is shown in chapter III.

## 4.2 Ocular Surgery

New surgical techniques in ophthalmology, such as phaco-emulsification for cataract surgery and laser corneal refractive surgery with increasing technical demands have stimulated, among others, the advance of new techniques for optical evaluation.

### *Corneal laser refractive surgery*

Different techniques, photorefractive keratectomy (PRK<sup>85</sup>), lasik in situ keratomileusis (LASIK<sup>86</sup>) or laser epithelial keratomileusis (LASEK<sup>87</sup>), are currently used as corneal laser correction methods. All of these techniques are based on corneal tissue removal using laser ablation in order to change corneal shape sufficiently to modify corneal optical power, decreasing it in a myopic correction or increasing it in a hyperopic correction. While, in PRK, laser ablation is done directly on the corneal first surface, in LASIK a hinged flap is created with a microkeratome and laser ablation is performed on the stroma. LASEK is a variant of PRK-LASIK where the flap is created with a finer blade instead of with a microkeratome. Early studies, following RK (radial keratectomy) and PRK, reported an increase of corneal aberrations compared to normal subjects<sup>88, 89</sup>. The first measurements of ocular aberrations changes<sup>89, 90</sup> with myopic LASIK showed that, despite the fact that myopia and astigmatism were in general successfully corrected, the procedure induced an increase of total higher order aberrations, and particularly a change of spherical aberration toward more positive values. This thesis presents a detailed study evaluating the contribution of corneal and internal aberrations to the aberration changes induced by LASIK surgery (chapter V)<sup>91</sup>.

Aberration techniques have been crucial to promote improvements of LASIK surgery, and in particular to help to identify problems inherent to the current techniques. It has been reported that the experimental changes in spherical aberration measured after LASIK myopic surgery are not due to standard algorithm (Munnerlyn) itself<sup>92-94</sup>, but to the actual application of the ablation profile, the laser-efficiency changes across the cornea,<sup>94, 95</sup> or the biomechanical responses of the cornea<sup>96</sup>.

Optical changes with myopic LASIK have been better studied than hyperopic LASIK. To our knowledge, the first study of combined aberrometry in changes of aberrations for this type of surgery has been done by Llorente et al<sup>97</sup> using the

techniques developed in the current thesis, on a group of 13 eyes finding a significant increase of higher order aberrations, specially in spherical aberration toward negative values (in myopic LASIK spherical aberration induced is toward positive values<sup>91</sup>).

### ***Cataract surgery***

Following the World Health Organisation estimations<sup>98</sup> there are over 19 million people blind as a result of cataract, being to date no effective treatment other than the surgery. The first cataract surgeries involved extracting the opacified compact crystalline lens: nucleus-cortex and capsule (intracapsular technique), or preserving the capsule (extracapsular technique). More recently the use of ultrasound or laser to break the crystalline in small pieces not affecting the capsule, named phacoemulsification, and the use of foldable intraocular lenses (IOL), has allowed to reduce significantly the incision sizes<sup>99</sup>. In addition to the advances in surgery techniques new designs of IOLs have appeared in the last years (see section 4.3).

Corneal topography has revealed the optical effects of the corneal incision in phacoemulsification, specially measuring changes in corneal astigmatism related to the different localization or shape of the incision<sup>100, 101</sup>. *In vivo* evaluation of the global optical performance of subjects who have undergone cataract surgery had only been done by means of double-pass techniques, where the MTF is measured<sup>102-104</sup> with results showing a decrease of optical quality in eyes implanted with IOLs with respect to young eyes. However a more complete description is given by optical measurement of wave aberrations. To our knowledge, we have used for the first time combined measurements of total and corneal aberrations in cataract surgery to provide aberrations of the IOL *in vivo*<sup>105</sup>. Results are shown in chapter VII.

### **4.3 Ophthalmic lenses design and testing**

Spectacle, contact and intraocular lenses are commonly used to correct for refractive errors. The developed technology in this thesis is promising to evaluate standard corrections and devise improved and customized systems.

### ***External lenses: Spectacle and contact lenses***

Conventional spectacle lenses correct for myopia and astigmatism (low order aberrations). Current efforts are directed to design customized lenses, which would correct also high order aberrations of individual eyes<sup>106</sup>. A customized lens will obviously require accurate measurements of aberrations before it is manufactured based on the individual wave aberrations. The measurement of aberrations has also provided estimable help in understanding the optical implementation of ophthalmic and contact lenses on real eyes<sup>107, 108</sup>. Aberrations measurements have allowed the evaluation of interesting issues that theoretical analysis, using computer modeling, is unable to show<sup>109, 110</sup>. Examples of these factors are the effects of internal aberrations, lens flexure or of the “tear film lens” in optical performance in Rigid Gas Permeable contact lenses wearers<sup>107</sup>. This study will be presented in chapter VI.

### ***Intraocular lenses***

Nowadays a great variety of intraocular lenses (IOLs) are available for cataract and even refractive surgery. They can be classified either by the material they are made: silicone, acrylic or poly-methyl methacrylate (PMMA), the geometric design: biconvex, plano-convex, meniscus or the optical properties: monofocal, bifocal, multifocal, or diffractives. The newest designs try not only to provide the optimal focal length but also try to correct spherical aberration by aspheric surfaces designs<sup>111</sup>.

Optical quality of implanted IOLs is usually tested outside the eye, *in vitro*, by interferometric methods, Modulation Transfer Function (MTF) measurements, or resolution methods<sup>112, 113</sup>. In chapter VII, we will present a laser ray tracing technique to evaluate wave aberrations of IOL *in vitro*, and to compare results with *in vivo* measurements and simulated ray tracing on manufacturer design data.

## **5. Goals of this thesis**

The main goal of this research is the implementation of a methodology to estimate corneal aberrations in the human eye which, in combination with total aberrometry, will be used to understand the contribution of the different ocular components to overall optical quality in the eye. They will be used, in particular, to test biological situations

and the changes induced by different surgical and non-surgical refractive correction methods. A detailed description of the methodology is presented in chapter II.

The specific goals of this thesis are:

1. To study the accuracy and precision of the implemented corneal and total aberrometry techniques (Chapter II).

2. Cross-validation of corneal based on Placido Disk corneal topography aberrometry and total ray tracing aberrometry to estimate corneal and total aberrations in real eyes. Correspondences of total and corneal aberrations on eyes with predominantly corneal aberrations (i.e. keratoconus, chapter III) or with no crystalline lens (i.e. aphakic eyes, chapter IV) will be tested.

3. Estimation of the optical performance of eyes with keratoconus corneal pathology, and the predominant type of aberration in these eyes (chapter III).

4. To study the ocular optics in both eyes of a unilateral aphakic young patient. Measurement of corneal and total aberrations in the normal eye, as opposed to the eye with no crystalline lens, will provide information on the total/corneal interaction. Measurements in the aphakic eye will allow to discuss possible effects of the posterior corneal surface (Chapter IV)

5. Description of total and corneal aberrations in young myopes, pre-operative patients of a myopic LASIK study and young control group for an aging/IOL eye study (Chapters V & VII).

6. Investigation of the optical changes induced on the cornea and total eye by myopic LASIK surgery. The study of changes in the internal optics will allow us to draw conclusions on the changes of the posterior corneal surface after LASIK. (Chapter V).

7. To study the potential of Rigid Gas Permeable (RGP lenses) to correct ocular aberrations, by measuring total and anterior surface aberrations on the same patients with and without RGP contact lenses. (Chapter VI).

8. Investigation of the sources of aberrations in patients after cataract surgery: changes in corneal aberrations by the incision, aberrations of standard intraocular lenses and their interaction with the patients' corneal aberrations. *In vivo* measurements will be compared to *in vitro* measurements on the same lenses and computer simulations using eye modelling (Chapter VII).

9. Development of an optimization methodology to estimate the gradient index structure of the crystalline lens in the human eye. Accuracy and possibilities of the technique will be tested by comparing results of the reconstruction of the gradient structure in a commercial lens with its known index distribution (Chapter VIII).

## 6. References

1. J. M. Bueno and P. Artal, "Polarization and retinal image quality estimates in the human eye," *J Opt Soc Am A* 18(3), 489-496 (2001).
2. S. Marcos, L. Diaz-Santana, L. Llorente, and C. Dainty, "Ocular aberrations with ray tracing and Shack-Hartmann wave-front sensors: Does polarization play a role?," *J Opt Soc Am A* 19(6), 1063-1072 (2002).
3. J. W. Goodman, *Introduction to Fourier optics* (New York, 1996).
4. W. S. Stiles and B. H. Crawford, "The luminous efficiency of rays entering the eye pupil at different points," *Proc. Roy. Soc.* 112, 428-450 (1933).
5. S. Marcos and S. A. Burns, "On the symmetry between eyes of wavefront aberration and cone directionality," *Vision Res* 40, 2437-2447 (2000).
6. W. J. Welford, *Aberrations of optical systems* (Adam Hilger Ltd, Bristol, England, 1986).
7. J. Casas, *Óptica* (Librería Pons, 1994 (Séptima Edición)).
8. G. Smith and D. A. Atchison, *The eye and visual optical instruments* (Cambridge University Press, 1997).
9. M. Born and E. Wolf, *Principles of Optics*, 6th ed. (Pergamon Press, Oxford, U.K., 1993).
10. D. Malacara, *Optical Shop Testing*, 2nd ed. ed. (Wiley, New York, 1992).
11. R. A. Applegate, L. N. Thibos, A. Bradley, S. Marcos, A. Roorda, T. O. Salmon, and D. A. Atchison, "Reference axis selection: Subcommittee report of the OSA working group to establish standards for measurement and reporting of optical aberrations of the eye," *J Refract Surg* 16, S656-S658 (2000).
12. H. Howland and B. Howland, "A subjective method for the measurement of monochromatic aberrations of the eye," *J. Opt. Soc. Am. A.* 67(11), 1508-1518 (1977).
13. F. Zernike, "Physica," 1:689 (1934).
14. L. N. Thibos, R. A. Applegate, J. T. Schwiegerling, R. Webb, and V. S. T. Members, "Standards for reporting the optical aberrations of eyes," *Vision Science and its Applications. Topics Volume* 35(2000).
15. R. J. Noll, "Zernike polynomials and atmospheric turbulence," *J Opt Soc Am A* 66, 207-311 (1976).
16. V. N. Mahajan, *Optical imaging and aberrations: Ray geometrical optics* (SPIE-The International Society for Optical Engineering, Washington, 1998), Vol. 1.
17. A. Guirao and D. R. Williams, "A method to predict refractive errors from wave aberration data," *Optom Vis Sci* 80, 36-42 (2003).
18. F. Flamant, "Étude de la repartition de lumière dans l'image rétinienne d'une fente," *Rev Opt Theor Instrum* 34, 433-450 (1955).
19. J. Santamaria, P. Artal, and J. Bescós, "Determination of the point-spread function of human eyes using a hybrid optical-digital method," *J. Opt. Soc. Am. - A* 4, 1109-1114 (1987).
20. P. Artal, R. Navarro, S. Marcos, and D. R. Williams, "Odd aberrations and double-pass measurements of retinal image quality," *J. Opt. Soc. Am. A.* 12(2), 195-201 (1995).
21. I. Iglesias, E. Berrio, and P. Artal, "Estimates of the ocular wave aberration from pairs of double-pass retinal images," *J- Opt. Soc. Am. A.* 15(9), 2466-2476 (1998).
22. L. Diaz-Santana, "Wavefront sensing in the human eye with a Shack-Hartmann sensor," (University of London, London, 2000).
23. F. Berny, "Etude de la formation des images rétiniennes et détermination de l'aberration de sphéricité de l'oeil humain," *Vision Res.* 9, 977-990 (1969).
24. T. Young, "On the mechanisms of the eye," *Phil. Trans. R. Soc.* 19, 23-88 (1801).

25. A. Ivanoff, *Les aberrations de l'oeil. Leur role dans l'accommodation*, Éditions de la revue d'Optique Théorique et Instrumentale (Masson & Cie., Éditeurs, 1953).
26. M. S. Smirnov, "Measurement of the wave aberration of the human eye," 776-795 (1961).
27. M. Tscherning, "Die monochromatischen aberrationen des menschlichen auges," *Z Physiol Sinne* 6, 456-471 (1894).
28. R. H. Webb, C. M. Penney, and K. P. Thompson, "Measurement of ocular wavefrontdistortion with a spatially resolved refractometer," *Appl. Opt.* 31, 3678-3686 (1992).
29. J. C. He, S. Marcos, R. H. Webb, and S. A. Burns, "Measurement of the wave-front aberration of the eye by a fast psychophysical procedure," *J. Opt. Soc. Am. A.* 15(9), 2449-2456 (1998).
30. R. Navarro and M. A. Losada, "Aberrations and relative efficiency of light pencils in the living human eye," *Optom Vis Sci* 74, 540-547 (1997).
31. V. V. Molebny, I. G. Pallikaris, L. P. Naoumidis, I. H. Chyzh, S. V. Molebny, and V. M. Sokurenko, "Retina ray-tracing technique for eye refraction mapping," presented at the Proc SPIE, 1997.
32. G. Walsh, W. N. Charman, and H. C. Howland, "Objective technique for the determination of monochromatic aberrations of the human eye," *J Opt Soc Am A* 1(9), 987-992 (1984).
33. B. Howland, "Use of Crossed Cylinder Lens in Photographic Lens Evaluation," *Applied Optics* 7(8), 1587-1599 (1968).
34. P. Mierdel, H. E. Krinke, W. Wiegand, M. Kaemmerer, and T. Seiler, "A measuring device for the assessment of monochromatic aberrations in human eyes," *Ophthalmologie* 94, 441-445 (1997).
35. J. Liang, B. Grimm, S. Golez, and J. Bille, "Objective measurement of wave aberrations of the human eye with the use of a Hartmann-Shack wave-front sensor," *J Opt Soc Am A* 11(7), 1949-1957 (1994).
36. E. Javal, *Mémoires d'ophtalmométrie* (G Masson, Paris, 1890).
37. R. B. Mandell and R. St Helen, "Mathematical model of the corneal contour," *Br J Physiol Opt* 26, 183-197 (1971).
38. M. Guillon, D. P. M. Lydon, and C. Wilson, "Corneal topography: a clyncial model," *Ophthal Physiol Opt* 6, 47-56 (1986).
39. M. Dubbelman, H. A. Weeber, R. G. Van der Heijde, and H. J. Volker-Dieben, "Radius and asphericity of the posterior corneal surface determined by corrected Scheimpflug photography," *Acta Ophthalmol Scand* 80(4), 379-383 (2002).
40. Y. Mejía-Barbosa and D. Malacara-Hernández, "A review of methods for measuring corneal topography," *Opt Vis Sci* 78, 240-253 (2001).
41. G. Westheimer, "Image quality in the human eye," *Opt Acta* 17, 641-658 (1970).
42. D. A. Atchison and G. Smith, eds., *Optics of the human eye* (Butterworth-Heinemann, 2000).
43. H. L. Liou and N. A. Brennan, "Anatomically accurate, finite model eye for optical modelling," *J Opt Soc Am A* 14, 1684-1695 (1997).
44. S. Marcos, S. A. Burns, P. M. Prieto, R. Navarro, and B. Baraibar, "Investigating the sources of monochromatic aberrations and transverse chromatic aberration," *Vision Res* 41, 3862-3871 (2001).
45. J. C. Barry, M. Dunne, and T. Kirschkamp, "Phakometric measurement of ocular surface radius of curvature and alignment: evaluation of method with physical model eyes," *Ophthal Physiol Opt* 21(6), 450-460 (2001).
46. D. O. Mutti, K. Zadnik, and A. J. Adams, "A video technique for phakometry of the human crystalline lens," *Inv Opth Vis Sci* 33, 1771-1782 (1992).
47. G. Smith and L. F. Garner, "Determination of the radius of curvature of the anterior lens surface from the Purkinje images," *Ophthal Physiol Opt* 16(2), 135-143 (1996).
48. D. O. Mutti, L. A. Jones, M. L. Moeschberger, and K. Zadnik, "AC/A Ratio, Age, and Refractive Error in Children," *Invest. Ophthalmol. Vis. Sci.* 41(9), 2469-2478 (2000).
49. Z. Liu, A. J. Huang, and S. C. Pflugfelder, "Evaluation of corneal thickness and topography in normal eyes using the Orbscan corneal topography system," *Br J Ophthalmol* 83(7), 774-778 (1999).
50. S. Patel, J. Marshall, and F. Fitzke, "Shape and radius of posterior corneal surface," *Refract Corneal Surg* 9, 173-181 (1993).
51. M. Dubbelman and R. G. Van der Heijde, "The shape of the aging human lens: curvature, equivalent refractive index and the lens paradox," *Vision Res* 41, 1867-1877 (2001).



52. J. Porter, A. Guirao, I. G. Cox, and D. R. Williams, "The human eye's monochromatic aberrations in a large population," *J Opt Soc Am A* 18, 1793-1803 (2001).
53. L. N. Thibos, X. Hong, A. Bradley, and X. Cheng, "Statistical variation of aberration structure and image quality in a normal population of healthy eyes," *J Opt Soc Am A* 19(12), 2329-2348 (2002).
54. P. Vinciguerra, F. I. Camesasca, and A. Calossi, "Statistical analysis of physiological aberrations of the cornea," *J Refract Surg* 19(2 Suppl), S265-269 (2003).
55. S. Patel, J. Marshall, and F. Fitzke, "Refractive index of the human corneal epithelium and stroma," *J Refract Surg* 11, 100-106 (1995).
56. M. Dubbelman, R. G. Van der Heijde, H. A. Weeber, and G. F. J. M. Vrensen, "Changes in the internal structure of the human crystalline lens with age and accommodation," *Vision Res* 43, 2363-2375 (2003).
57. B. A. Moffat, D. A. Atchison, and J. M. Pope, "Age-related changes in refractive index distribution and power of the human lens as measured by magnetic resonance micro-imaging in vitro," *Vision Res* 42, 1683-1693 (2002).
58. M. Millodot and J. G. Sivak, "Contribution of the cornea and lens to the spherical aberration of the eye," *Vis Res* 19, 685-687 (1979).
59. P. Artal and A. Guirao, "Contribution of the cornea and the lens to the aberrations of the human eyes," *Opt Lett* 23, 1713-1715 (1998).
60. A. Tomlinson, R. P. Hemenger, and R. Garriott, "Method for Estimating the Spheric Aberration of the Human Crystalline Lens in Vivo," *Invest. Ophthalmol. & Vis. Sci.* 34(3), 621-629 (1993).
61. S. G. El Hage and F. Berny, "Contribution of the crystalline lens to the spherical aberration of the eye," *Journal of the Optical Society of America* 63, 205-211 (1973).
62. P. Artal, A. Guirao, E. Berrio, and D. R. Williams, "Compensation of corneal aberrations by the internal optics in the human eye," *J Vision* 1, 1-8 (2001).
63. P. Artal, E. Berrio, A. Guirao, and P. Piers, "Contribution of the cornea and internal surfaces to the change of ocular aberrations with age," *J Opt Soc Am A* 19, 137-143 (2002).
64. T. O. Salmon, "Corneal contribution to the wavefront aberration of the eye," (Indiana, 1999).
65. S. A. Burns, S. Marcos, A. E. Elsner, and S. Bara, "Contrast improvement for confocal retinal imaging using phase correcting plates," *Opt Lett* 27, 400-402 (2002).
66. A. Roorde, F. Romero-Borja, W. J. Donnelly, H. Queener, T. J. Hebert, and C. W. Campbell, "Adaptive optics scanning laser ophthalmoscopy," *Optics Express* 10(9), 405-412 (2002).
67. C. Owsley, R. Sekuler, and D. Siemsen, "Contrast sensitivity throughout adulthood," *Vision Res* 23, 688-699 (1983).
68. D. Elliott, D. Whitaker, and D. MacVeigh, "Neural contribution to spatio temporal contrast sensitivity decline in healthy ageing eyes," *Vision Res* 30, 541-547 (1990).
69. T. Van den Berg and J. K. Ijspeert, "Light scattering in donor lenses," *Vision Res* 35, 169-177 (1995).
70. R. Calver, M. Cox, and D. Elliott, "Effect of aging on the monochromatic aberrations of the human eye," *J Opt Soc Am A* 16(16), 2069-2078 (1999).
71. J. McLellan, S. Marcos, and S. A. Burns, "Age-related changes in monochromatic wave aberrations of the human eye," *Invest Ophthalmol Vis Sci* 42, 1390-1395 (2001).
72. A. Guirao, M. Redondo, and P. Artal, "Optical aberrations of the human cornea as a function of age," *J Opt Soc Am A* 17, 1697-1702 (2000).
73. A. Glasser and M. Campbell, "Biometric, optical and physical changes in the isolated human crystalline lens with age in relation to presbyopia," *Vis. Res.* 39, 1991-2015 (1999).
74. G. Smith, M. J. Cox, R. Calver, and L. F. Garner, "The spherical aberration of the crystalline lens of the human eye," *Vision Res* 41, 235-243 (2001).
75. D. Goss, H. G. Van Veen, B. B. Rainey, and B. Feng, "Ocular components measured by keratometry, phakometry, and ultrasonography in emmetropic and myopic optometry students," *Optom Vis Sci* 74, 489-495 (1997).
76. J. Wallman, *Retinal factors in myopia and emmetropization: clues from research on chicks*, *Refractive Anomalies: Research and Clinical Applications* (Butterworth-Heinemann, Boston, 1991), pp. 235-245.
77. M. J. Collins, C. F. Wildsoet, and D. A. Atchison, "Monochromatic aberrations and myopia," *Vision Res* 35(9), 1157-1163 (1995).
78. S. Marcos, E. Moreno-Barriuso, L. Llorente, R. Navarro, and S. Barbero, (personal communication).

79. J. C. He, J. Gwiazda, R. Held, and F. Thorn, "Wavefront aberrations in the cornea and whole eye for emmetropes and myopes," *Invest Ophthalmol Vis Sci* (suppl) 542(2001).
80. G. Carney, J. C. Mainstone, and B. A. Henderson, "Corneal topography and myopia: A cross-sectional study," *Inv Oph Vis Sci* 38, 311-320 (1997).
81. S. Marcos, S. Barbero, and L. Llorente, "The sources of optical aberrations in myopic eyes," presented at the *Inv Oph Vis Sci*, (Suppl.)42,133,(2001) Fort Lauderdale, Florida, USA, 2002.
82. J. Schwiegerling, "Cone Dimensions in Keratoconus using Zernike polynomials," *Optom Vis Sci* 74(Keratoconus), 963-969 (1997).
83. M. A. Lagana, I. G. Cox, and R. J. Potvin, "The effect of keratoconus on the wavefront aberration of the human eye," *Invest Ophthalmol Vis Sci* (suppl) 41, S679 (2000).
84. S. Barbero, S. Marcos, J. Merayo-Llodes, and E. Moreno-Barriuso, "A validation of the estimation of corneal aberrations from videokeratography: test on keratoconus eyes," *J Refract Surg* 18, 267-270 (2002).
85. M. B. McDonald, J. C. Liu, and T. J. Byrd, "Central photorefractive keratectomy for myopia: partially sighted and normally sighted eyes," *Ophthalmology* 98, 1327-1337 (1991).
86. I. G. Pallikaris, M. Papatzanaki, E. Stathi, O. Frenschock, and A. Georgiadis, "Laser in situ keratomileusis," *Lasers Surg Med* 10, 463-468 (1990).
87. M. H. Dastjerdi and H. K. Soong, "LASEK (laser subepithelial keratomileusis)," *Curr Opin Ophthalmol* 13(4), 261-263 (2002).
88. M. W. Campbell, H. Haman, P. Simonet, and I. Brunette, "Dependence of optical image quality on refractive error: eyes after excimer laser photorefractive keratectomy (prk) versus controls," *Invest. Oph.& Vis. Sci.* 40 (Suppl.)4, s7 (1999).
89. T. Seiler, M. Kaemmerer, P. Mierdel, and H.-E. Krinke, "Ocular optical aberrations after photorefractive keratectomy for myopia and myopic astigmatism," *Arch Ophthalmol* 118, 17-21 (2000).
90. E. Moreno-Barriuso, J. Merayo-Llodes, S. Marcos, R. Navarro, L. Llorente, and S. Barbero, "Ocular aberrations before and after corneal refractive surgery: LASIK-induced changes measured with Laser Ray Tracing," *Invest Ophthalmol Vis Sci* 42, 1396-1403 (2001).
91. S. Marcos, S. Barbero, L. Llorente, and J. Merayo-Llodes, "Optical Response to Myopic LASIK Surgery from Total and Corneal Aberration Measurements," *Invest Ophthalmol Vis Sci* 42, 3349-3356 (2001).
92. J. Jiménez, R. Anera, and L. Jiménez del Barco, "Equation for corneal asphericity after corneal refractive surgery," *J Refract Surg*, 65-69 (2003).
93. C. Dorrnsoro, D. Cano, S. Barbero, J. Merayo, L. Llorente, and S. Marcos, "Understanding the standar algorithm for corneal refractive surgery using laser ablation of PMMA surfaces," presented at the E-abstract 2535, 2003.
94. D. Cano, S. Barbero, and S. Marcos, "Computer application of laser ablation patterns on real corneas and comparison with surgical outcomes," *J Opt Soc Am A* (Submitted).
95. J. R. Jiménez, R. Anera, L. Jiménez del Barco, and E. Hita, "Effect on laser ablation algorithms of reflection losses and nonnormal incidence on the anterior cornea," *Appl Phys Lett* 81(8), 1521-1523 (2002).
96. M. Asejczyk-Widlicka, W. Srodka, and H. Kasprzak, "The modelling of effect of refractive surgery on the physically linear model of human eyeball. Influence of IOP on the geometrical and biomechanical properties of the model of the eye globe.," presented at the MOPANE, 2003.
97. L. Llorente, S. Barbero, J. Merayo, and S. Marcos, "Changes in total and corneal aberrations induced by LASIK surgery for hyperopia," *J Refract Surg* (Submitted).
98. C. Hammond, "The epidemiology of cataract," (2001).
99. D. T. Azar, *Intraocular lenses in cataract and refractive surgery* (W.B. Saunders Company, Philadelphia, 2001).
100. T. Oshika, G. Sugita, T. Tanabe, A. Tomidokoro, and S. Amano, "Regular and irregular astigmatism after superior versus temporal scleral incision cataract surgery," *Ophthalmology* 107, 2049-2053 (2000).
101. T. Kohnen, B. Dick, and K. Jacobi, "Comparison of the induced astigmatism after temporal clear corneal tunnel incisions of different sizes," *J Cataract Refract Surg* 21(4), 417-424 (1995).
102. R. Navarro, M. Ferro, P. Artal, and I. Miranda, "Modulation transfer functions of eyes implanted with intraocular lenses," *App Opt* 32, 6359-6367 (1993).

103. P. Artal, S. Marcos, R. Navarro, I. Miranda, and M. Ferro, "Through focus image quality of eyes implanted with monofocal and multifocal intraocular lenses," *Optical Engineering* 34, 772-779 (1995).
104. A. Guirao, M. Redondo, E. Geraghty, P. Piers, S. Norrby, and P. Artal, "Corneal optical aberrations and retinal image quality in patients in whom monofocal intraocular lenses were implanted," *Archives of Ophthalmology* 120, 1143-1151 (2002).
105. S. Barbero, S. Marcos, and I. Jiménez-Alfaro, "Optical aberrations of intraocular lenses measured in vivo and in vitro," *J. Opt. Soc. Am. A* 20(10), 1841-1886 (2003).
106. N. Lopez-Gil, J. F. Castejón-Mochón, A. Benito, J. M. Marín, G. Lo-a-Foe, G. Marin, B. Fermigier, R. Renard, D. Joyeux, N. Château, and P. Artal, "Aberration generation by contact lenses with aspheric and asymmetric surfaces," *J Refract Surg* 18, S603-S609 (2002).
107. C. Dorronsoro, S. Barbero, L. Llorente, and S. Marcos, "Detailed on-eye measurement of optical performance of rigid gas permeable contact lenses based on ocular and corneal aberrometry," *Opt Vis Sci* 80(2), 115-125 (2003).
108. X. Hong, N. Himebaugh, and L. N. Thibos, "On-eye evaluation of optical performance of rigid and soft contact lenses," *Optom Vis Sci* 78, 872-880 (2001).
109. C. E. Campbell, "The effect of spherical aberration of contact lenses to the wearer," *Am J Optom Physiol Opt* 58, 212-217 (1981).
110. D. A. Atchison, "Aberrations associated with rigid contact lenses," *J Opt Soc Am A* 12, 2267-2273 (1995).
111. J. T. Holladay, P. A. Piers, G. Koranyi, M. Van der Mooren, and N. E. Norrby, "A new intraocular lens design to reduce spherical aberration of pseudophakic eyes," *J Refract Surg* 18(6), 683-691 (2002).
112. M. J. Simpson, "Optical quality of intraocular lenses," *J Cataract Refract surg* 18, 86-94 (1992).
113. V. Portney, "Optical testing and inspection methodology for modern intraocular lenses," *J Cataract Refract Surg* 18, 607-613 (1992).